



# Large scale structure of planetary environments: the importance of not being Maxwellian

Nicole Meyer-Vernet\*

*Département de Recherche Spatiale, CNRS UMR-8632, Observatoire de Paris, 92195 Meudon Cedex, France*

Received 15 December 1999; received in revised form 10 April 2000; accepted 17 May 2000

## Abstract

The velocity distributions observed in space have too many fast particles, by Maxwell's standards. This ubiquitous property raises doubts about the validity of models based on a set of fluid equations whose closure requires the distributions to be nearly Maxwellian. I discuss here two generic cases: bound structures and winds. Near rapidly rotating magnetised planets, particles channelled along co-rotating magnetic field lines are acted on by the field-aligned component of the centrifugal force, which exceeds the gravitational attraction beyond a few planetary radii. With dipolar magnetic fields, this tends to trap particles near the equator and produce torus-shaped structures, whereas gravitational confinement occurs closer to the planet. These confining forces act as high-pass filters for particle speeds, so that the temperatures are rising with distance from the potential wells, if the velocity distributions are not Maxwellian — in sharp contrast to classical isothermal equilibrium; and the density profiles fall off less steeply than a Gaussian — just as the velocity distributions fall off less steeply than a Maxwellian. While these bound structures are shaped along closed magnetic field lines, winds can blow along open field lines. A suprathermal tail in the electron velocity distribution increases the electric field which ensures the balance of ion and electron fluxes, and should thus increase the wind speed above the value predicted by classical hydrodynamic escape. © 2001 Elsevier Science Ltd. All rights reserved.

*Keywords:* Magnetospheres; Winds; Kinetic theory; Solar system plasmas

## 1. Introduction

“Let us consider our data”, Sherlock Holmes tells us (Doyle, 1927).

In 1992, the spacecraft Ulysses crossed Jupiter's magnetosphere from north to south, thereby providing the first — and to date, unique — in situ measurement of the latitudinal structure of the torus of plasma associated with the satellite Io. The electron temperature was found to rise strongly with latitude, whereas the density decrease was not Gaussian (Meyer-Vernet et al., 1993; Moncuquet et al., 1995), in clear contradiction with the current models (Bagenal, 1994).

These empirical models were in fact mere extrapolations of equatorial data, since Ulysses was the first probe leaving the vicinity of the Jovian equator — a serendipitous gift due to the exploration of the polar solar wind. Could these models be wrong? The culprit could not be a temperature anisotropy since this would have produced a temperature

variation much smaller than observed, and in the opposite sense. Neither could it be the high-energy electron component, since the measured temperature concerned explicitly the low-energy part. The data were obtained at variable longitudes, so could the culprit be a longitudinal asymmetry? Since the temperature increase was found to be roughly symmetrical in (centrifugal) latitude, such an explanation would have required that the temperature variation with longitude be tailored to fit, just in phase with the spacecraft trajectory (and anyway, not in line with the current data and theoretical schemes.)

What would William of Ockham have made of this? Minimising the hypotheses suggested to question instead a basic ingredient of the models: Maxwellian velocity distributions for each particle species—equivalent to diffuse equilibrium with uniform temperatures along magnetic field lines. Indeed, this assumption was in no way supported by observation. The velocity distributions were badly determined in the Io torus, because the electron measurements on Voyager were affected by the spacecraft potential, and the ion ones were complicated by confusion between particle species and by transonic speeds; for diverse reasons, the detailed Jovian

\* Tel.: +33-1-45-07-76-90; fax: +33-1-45-07-28-06.

E-mail address: nicole.meyer@obspm.fr (N. Meyer-Vernet).

exploration by the sophisticated Galileo spacecraft does not seem to have clarified the picture. Be that as it may, the data suggested non-Maxwellian distributions — as is generally observed in space plasmas, and as could be expected with so many non-equilibrium processes at work and so few collisions. Thus there was no reason — except of convenience — to assume Maxwell distributions.

“Once your point of view has changed”, Sherlock Holmes continues, “the very thing which was so damning becomes a clue to the truth”. Indeed, a non-Maxwellian velocity distribution is just what is needed to produce a temperature increase along field lines and a non-Gaussian density profile in a bound and collisionless environment, as Scudder (1992) showed in a quite different context. This is because the attractive force filters the particles by letting only the fast ones escape, thereby making the temperature rise outwards; this does not happen with a Maxwell distribution because in that case the filtration just multiplies the distribution by the Boltzmann factor, so that all particles are filtered similarly.

Indeed, simply discarding the Maxwellian hypothesis by taking into account a suprathermal electron tail compatible with the data enabled one to explain the Ulysses observations (Meyer-Vernet et al., 1995). And this novel point of view shortly turned out to remove a number of apparent inconsistencies in the Voyager and ground-based data (Moncuquet, 1997; Thomas and Lichtenberg, 1997).

These effects are clearly outside the scope of the classic fluid scheme, but they have important consequences on the large-scale structure of bound environments — in contrast to the widespread idea that kinetic effects play a role only at small scales. We will see that the consequences on winds are more subtle, albeit no less important. I discuss below the basic underlying physics for the generic cases of bound structures and of winds; at the risk of gross oversimplifications, I will keep things relatively simple in order to avoid the fundamental ideas being lost in the wealth of details and mathematics.

## 2. Suprathermal tails

As mentioned above, the velocity distributions observed in space are not in equilibrium: they are nearly Maxwellian at low energies, but they have an excess of fast particles which generally decreases as a power law (Fig. 1). This ubiquity of suprathermal tails has prompted a number of investigations along many fronts (see Scudder and Olbert, 1979; Collier, 1993; Treumann, 1999), but to date, nobody has come up with a full generic explanation. Be that as it may, such distributions are not surprising given the nature of particle “collisions” in plasmas, which do not occur as billiard balls, but rather via the Coulomb force; for two particles to interact significantly, they must come closer than the distance  $r$  at which the Coulomb potential ( $\propto 1/r$ ) equals the kinetic energy, so that their cross-section varies as the

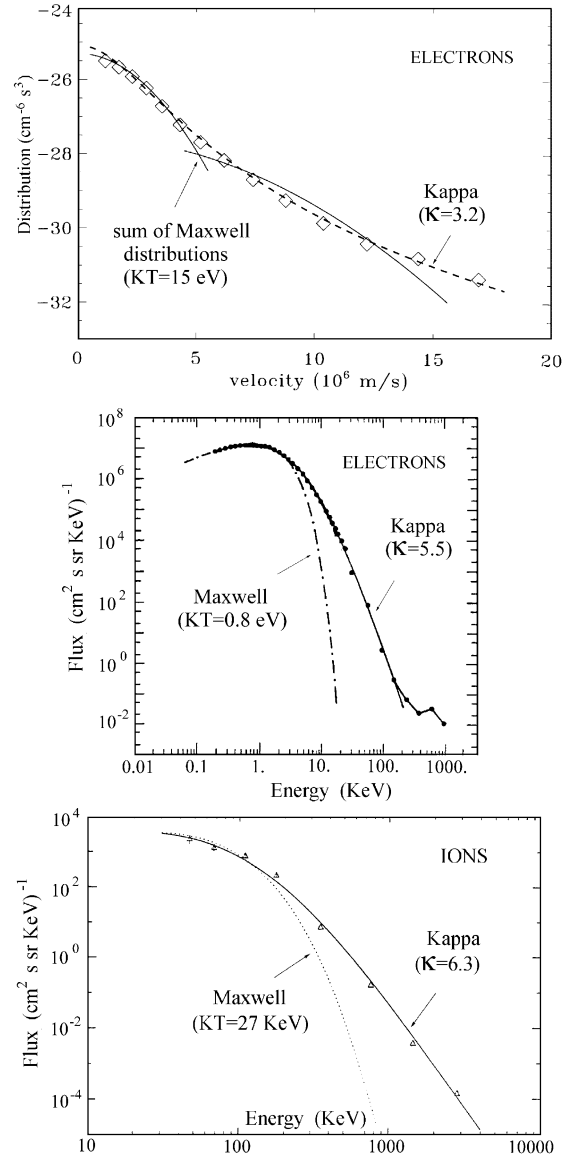


Fig. 1. Examples of velocity distributions observed in space, and comparison with Maxwellian and Kappa functions. Top: Electron distribution observed in the solar wind on Ulysses (adapted from Maksimovic et al., 1997a). Middle: Electron distribution observed in the Earth’s plasma sheet (Christon et al., 1988) (adapted from Pierrard, 1997). Bottom: Ion distribution observed in Saturn’s magnetosphere with the LECP instrument on Voyager 1 (adapted from Maurice, 1994).

inverse square of the energy (Spitzer, 1962). Thus a particle moving, say, three times faster than average has a free path greater by two orders of magnitude. Therefore, even though low-energy particles are often collisional, faster ones are generally not so; they are thus easily driven out of equilibrium and escape to large distances (Scudder and Olbert, 1979; Shoub, 1983).

How to model such distributions? In the menagerie of mathematical functions, the generalised Lorentzian

$$f(v) \propto \left[ 1 + \frac{v^2}{\kappa w^2} \right]^{-(\kappa+1)} \quad (1)$$

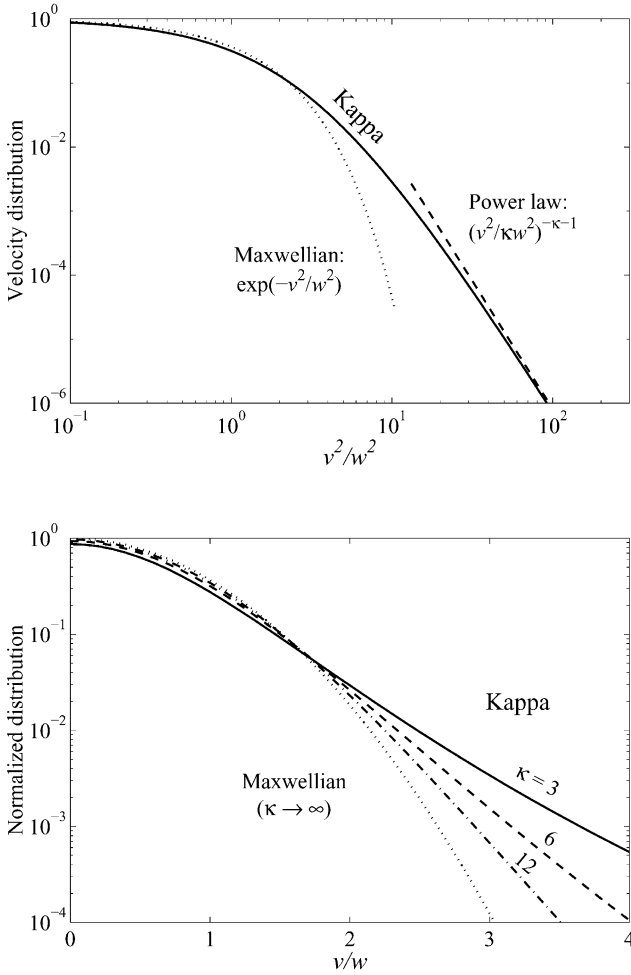


Fig. 2. Top: Kappa velocity distribution (Eq. (1) with  $\kappa=3$ ), compared to a Maxwellian and to a power law. Bottom: A series of Kappa distributions with different values of  $\kappa$ . All distributions are rather similar at speeds below the most probable speed  $w$ , but the smaller the value of Kappa, the more fast particles, and therefore the greater the kinetic temperature. The distributions are normalised so that they have the same number density (and the same most probable speed); the excess of suprathermal particles is compensated by a deficit in low-energy ones.

seems to do nicely. At speeds  $v \leq w$ , this so-called “Kappa” distribution is close to a Maxwellian ( $\propto e^{-v^2/w^2}$ ) of temperature  $T_\infty = mw^2/2k_B$  for particles of mass  $m$ , and it has a suprathermal power-law tail, in agreement with observation (Vasyliunas, 1968) (Fig. 2, top). The larger the value of  $\kappa$ , the lesser suprathermal particles, so that the distribution ultimately approaches the above Maxwellian as  $\kappa \rightarrow \infty$ ; it thus has the agreeable property of including the Maxwell distribution as a limiting case. The most probable speed is  $w$  whatever the value of  $\kappa$ ; but the kinetic temperature, given by  $m\langle v^2 \rangle / 3k_B$  (where the angular brackets denote a mean over the distribution) is  $T_\infty \times \kappa / (\kappa - 3/2)$ , and thus increases as  $\kappa$  decreases — due to the increasing size of the tail (Fig. 2, bottom). Hence,  $\kappa$  is constrained by the inequality  $\kappa > 3/2$  for the temperature to remain finite; in practice, it generally lies in the range 2–6. It may be noted that this function must

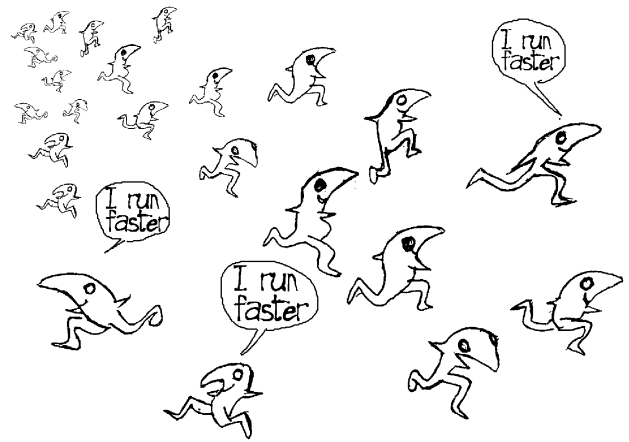
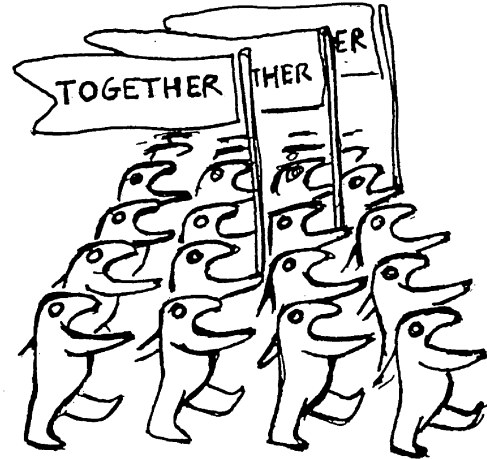


Fig. 3. Top: The classical fluid models require the particles to keep some spatial local ordering, and they assume nearly Maxwellian velocity distributions. Bottom: Space plasmas contain an excess of fast particles which do not interact locally since they are virtually collisionless; thus they may not behave as bona fide fluids (based on drawings from F. Meyer.)

be handled with care because it has only a limited number of finite moments. Although it is not the panacea, this function is one of the most suitable tools available for modelling velocity distributions observed in space.

Let us now consider this other pillar of large-scale modelling: the fluid approach.

### 3. Fluid or kinetic?

Why should the conventional fluid models be often inadequate in space plasmas for describing large-scale structures? After all, these structures contain so many particles that they should follow the average.

The fundamental reason can be understood intuitively in two ways. Firstly, the fluid models require the particles to be localised in space, so as to behave as a whole (Fig. 3, top). Indeed, if the medium is to be described by

differential equations, the rates of change must depend only on the local variables. Intuitively, this localisation requires the particles to travel less than a scale height before coming into equilibrium. But in most space plasmas, which contain an excess of virtually collisionless fast particles, the localisation processes are insufficient; it is often argued that the particle gyration in the magnetic field comes to the rescue for ensuring a fluid behaviour, but this does not act in the direction parallel to the field lines. Hence the medium might not behave as a bona fide fluid (Fig. 3, bottom). The other way is to note that *if* a fluid element is to be completely defined by its number of particles, velocity and energy, then the particle velocities should be distributed randomly around the average, that is, the velocity distribution should be Maxwellian; any other distribution would mean that more information is available (see Fort et al., 1999). As we have seen, space plasmas generally have non-Maxwellian distributions, so that a few macroscopic parameters may not carry enough information to describe them adequately.

It is not easy to put these intuitive feelings on a firmer basis, because the path leading from the kinetic plasma description to the small set of equations used in fluid models is tortuous and full of mines (see Montgomery and Tidman, 1964). It is fair to say that the problem is far from being solved, except in a few cases which rarely occur in space.

In the precise — albeit obtained itself from approximation — kinetic Boltzmann's scheme, the plasma is defined by the particle velocity distributions as functions of space and time. The passage to a fluid description — where the medium is more loosely defined by a few macroscopic parameters — involves truncating (at which level?) and closing (how?) an infinite set of coupled equations relating an infinite number of velocity moments. The simplest procedure uses only conservation of mass and momentum; since these two equations involve three parameters (density, velocity and pressure), the system is closed by assuming a relation between pressure and density; for example, if the changes are sufficiently slow to secure a uniform temperature bath, the pressure is proportional to the density; if, on the contrary, the changes are too fast to allow any heat exchange, the pressure is proportional to the density to the power  $5/3$  — the adiabatic relation for particles having three degrees of freedom. Both approximations require the velocity distributions to be sufficiently close to Maxwellian ones. A different approximation is sometimes used when the magnetic field is strong and collisions are rare, so that the medium is gyrotropic with different pressures in the directions parallel and perpendicular to the magnetic field: *if* heat transport is negligible, the adiabatic relation can then be generalised. In general, however, neither of these simple extremes holds, and heat transport must be taken into account explicitly.

Just as suggested by our intuitive feeling, the standard procedure for passing to such a fluid description involves an expansion into the ratio of the *mean* free path for scattering to the scale at which parameters vary — the so-called

“Knudsen number” (see Hinton, 1983 and references therein) (as mentioned above, the scale length to be compared to the free path may be the one in the direction parallel to the magnetic field). In ordinary gases, this expansion only requires that the Knudsen number be smaller than unity. But in plasmas, the criterion is more stringent and the Knudsen number must be *much* smaller than unity — which rarely holds in practice (see Scudder, 1992 and references therein). Why is this so? The fundamental reason is once more the steep increase of the free path with speed: even when the free path is small for “thermal” particles, it is not so for faster ones, thereby precluding uniform convergence of the expansion, as has been recognised in earnest some time ago (see Scudder and Olbert, 1979; Scudder and Olbert, 1983; Shoub, 1983).

It is not surprising that the fluid approximations become questionable when the velocity distributions have suprathermal tails. Indeed, the heat flux — the third velocity moment — depends mainly on the fast particles: the faster the particles, the more efficiently they conduct heat; this is still truer for the higher-order moments which are disposed of in the fluid truncation and closure schemes: the higher the order of the moment, the larger the relative contribution of the fast particles, so that higher-order fluid theories may not be better.

We conclude from all this that the usual fluid models should be taken with a large pinch of salt: with few collisions and non-Maxwellian distributions, the classical schemes may be inadequate; in essence, they imply a local relationship, whereas the fast particles, which are virtually collisionless, make the problem non-local. Let us now examine some generic consequences on planetary environments.

#### 4. Trapping agents

Close to planets, which are generally rotating and magnetised, several effects conspire to confine the plasma. Particles are of course subjected to the planet's gravitational field, but they are also channelled by the magnetic field; in the region co-rotating with the planet, they are thus pulled towards the equator by the component of the centrifugal force acting along the field. One expects this force to be larger than the magnetic mirror force by about the ratio of the particle co-rotation energy (500 eV for oxygen at Io's orbit) to its thermal energy (see Cummings et al., 1980). Just as pearls threaded along a rotating wire (Fig. 4), particles moving along a field line tend to accumulate near the point where the **B**-aligned centrifugal component vanishes; this defines the so-called “centrifugal equator” (which is shifted off the magnetic equator when the planet's magnetic and spin axes do not coincide) (Gledhill, 1967).

Consider a very elementary model which contains the basic physics: a planet of mass  $M$  rotating with angular velocity  $\Omega$ , and having a dipolar magnetic field whose axis is aligned with the spin axis. Consider now a particle of mass

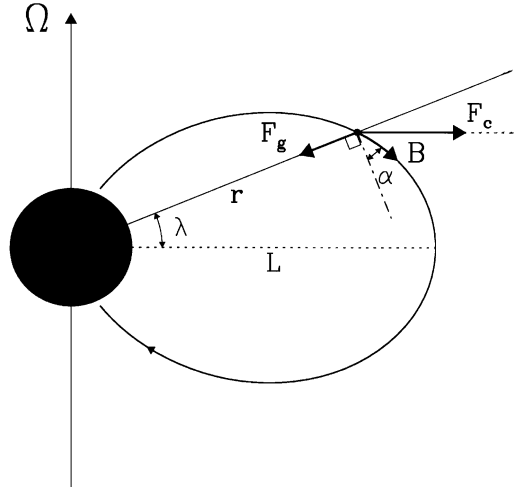


Fig. 4. Particles channelled by magnetic field lines are subjected to the projection on  $\mathbf{B}$  of the centrifugal force  $\mathbf{F}_c$  and of the gravitational force  $\mathbf{F}_g$ . The figure illustrates the simple case when the magnetic and spin axes coincide, so that the centrifugal component along  $\mathbf{B}$  tends to trap particles near the magnetic equator.

$m$  at distance  $r$  from the planet and latitude  $\lambda$ . With a dipolar magnetic field, the angle  $\alpha$  between  $\mathbf{B}$  and the normal to the radius vector is related to the latitude by  $\tan \alpha = 2 \sin \lambda$ . Now, the centrifugal force is given by  $F_c = m\Omega^2 r \cos \lambda$ , and its projection on  $\mathbf{B}$  equals  $F_c \sin(\lambda + \alpha)$  (Fig. 4). For small latitudes, one has  $\alpha \approx 2\lambda$ , so that the projected centrifugal force is roughly  $F_c \times 3\lambda$ , whence

$$F_{c||} \approx 3m\Omega^2 z \quad (2)$$

at small distances  $z \approx \lambda r$  from the equilibrium position. The particle is also subjected to the gravitational force  $F_g = mMG/r^2$  ( $G$  being the constant of gravitation), whose projection on  $\mathbf{B}$  is given by  $-F_g \sin \alpha \approx -2F_g z/r$ . The gravitational and centrifugal components are thus roughly equal at the distance

$$r_c = (2MG/3\Omega^2)^{1/3}. \quad (3)$$

This equatorial distance is in some sense akin to the ‘‘Roche limit’’ of neutral media: in this vicinity, a co-rotating plasma droplet tends to break into two pieces, one falling inwards along the magnetic field, while the other is pulled towards the centrifugal equator (see Lemaire, 1974, 1999; we will return to this point in Section 7). This distance amounts to about 6 planetary radii for the Earth, but to only 2 planetary radii for Jupiter and for the other outer planets. Indeed, gravitation dominates in the Earth’s plasmasphere, except when the solar wind induced electric field increases significantly the plasma rotational speed above co-rotation, thereby decreasing  $r_c$ . In contrast, the centrifugal component is the main trapping agent in the co-rotating region of outer planets (except at very short distances).

Let us study this case in a little more detail. Consider the generic example of Io’s plasma torus — a

structure surrounding Jupiter at about 6 Jovian radii. How far does it extend from the equilibrium centrifugal plane? Let us suppose that there is only one ion species, of mass  $m_i$  and uniform temperature  $T$ . We can guess that the particles fill the region where their centrifugal energy exceeds their thermal energy. With the centrifugal force (2) acting on ions of mass  $m_i$  (the light electrons barely feel it), the increase in potential energy at a (small) distance  $z$  is

$$W_c \approx 3m_i\Omega^2 z^2/2. \quad (4)$$

Equating this value to  $k_B T$  gives an estimate of the torus vertical extent on each side of the equilibrium plane

$$H = \left[ \frac{2k_B T}{3m_i\Omega^2} \right]^{1/2}. \quad (5)$$

Not unexpectedly, this is just the value derived from the isothermal (bi)-fluid approach (Gledhill, 1967) when the electron pressure is neglected. Indeed, the hydrodynamic ion pressure equation along  $\mathbf{B}$  yields

$$d p/dz = -n F_{c||}, \quad (6)$$

where  $n$  is the number density of ions. Now, let us assume *isothermal equilibrium* along field lines, i.e.  $T$  does not depend on  $z$ ; substituting the force (2) and the ion pressure  $p = nk_B T$  yields

$$dn/dz = -2nz/H^2 \quad (7)$$

whence

$$n \propto \exp(-z^2/H^2). \quad (8)$$

It may be worth noting that since the above calculation neglects the electron pressure, it contains the hidden assumption that the electron temperature is much smaller than the ion one. With equal temperatures, the total pressure would be twice greater (if the ions are singly charged, i.e. if there are as many ions as electrons), which yields a scale height greater by a factor of  $\sqrt{2}$  — a result which can also be obtained by putting the average particle mass (roughly half the ion one) in the scale height (5).

The canonical Gaussian profile found above is used in various contexts with modifications of detail. However, it involves a crucial assumption: isothermal equilibrium along field lines. We saw in the introduction that this assumption conflicts with observation, but it is not evident how to proceed instead if we stick to the fluid picture. What is the adequate closure relation? And is there any? So let us see what the kinetic theory has to tell us.

## 5. A kinetic picture of trapping

When the mean free paths are much greater than the scale heights, as occurred for Ulysses’ encounter, we may neglect collisions — a huge simplification, so that the velocity distribution of each particle species equals a constant following particle trajectories. Under the form of what is sometimes

called Jeans' theorem (Chandrasekhar, 1942), this means that we can calculate here the velocity distributions as functions of the constants of motion of the particle trajectories. In the spirit of our simple model, let us suppose that the distributions are isotropic in the frame rotating with the planet, so that they depend only of the value  $v$  of the velocity, but not on its direction. In this case, if the distribution of a particle species is  $f_0(v)$  at  $z = 0$ , then its value at altitude  $z$  is simply  $f(v) = f_0(v_0)$ , where the speeds  $v$  and  $v_0$  are related by energy conservation, that is,  $mv^2/2 + W = mv_0^2/2$ , where  $W$  is the increase in potential energy between the altitudes 0 and  $z$ ; this holds for particles of mass  $m$  following trajectories connecting these altitudes. Since particles are pulled towards the equator, all trajectories connect to  $z = 0$ , so that the velocity distribution is given by

$$f(v, z) = f_0[(v^2 + 2W/m)^{1/2}]. \quad (9)$$

A small but non-trivial aside is in order here. The value of the magnetic field does not enter explicitly because the distribution is isotropic, so that energy conservation is sufficient to calculate it. However, we have implicitly used the fact that the magnetic field is increasing with  $z$  — as the potential energy does — which ensures a simple mapping of particle orbits; we will return to this point in Section 7.

### 5.1. Keeping the plasma neutral

As already mentioned, the light electrons are hardly affected by the centrifugal component which pulls the ions towards the equator; the corresponding charge imbalance produces an electric field parallel to the magnetic lines, whose direction ensures that the electrons are also pulled towards the equator. This electric field adjusts itself for preserving charge quasi-neutrality. In the spirit of our simple model, let us suppose that both species have similar energy distributions at  $z = 0$  and opposite charges. The parallel electric force on the ions is then one-half of the centrifugal component and acts in the opposite direction; in this way, the total parallel force on ions is halved and is equal to the force acting on electrons. Consequently, the total potential energy of each species is just half the centrifugal potential (4)

$$W \approx W_c/2 \approx 3m_i\Omega^2 z^2/4. \quad (10)$$

Two comments are in order here. Firstly, if the situation were more complicated — as often occurs in practice — the electrostatic force would be a priori unknown, and should be calculated from the condition that the plasma must be quasi-neutral. Secondly, the electrostatic field is implicit in the hydrodynamic picture handling the plasma as a single (neutral) fluid. When electrons and ions are viewed as two separate (charged) fluids, the electric field serves to balance the electron pressure force: this yields the above value of the potential if the temperatures are equal.

### 5.2. Trapped Maxwell distributions

Let us assume Maxwell–Boltzmann distributions of temperature  $T$  at  $z = 0$ , that is

$$f_0(v) \propto \exp(-mv^2/2k_B T) \quad (11)$$

for a species of mass  $m$ . Eq. (9) tells us that the distribution at  $z$  is then given by

$$f(v, z) = \exp(-W/k_B T) \times f_0(v) \quad (12)$$

which is just the initial Maxwellian with the same temperature and a number density  $n$  multiplied by the Boltzmann factor:

$$n \propto \exp(-W/k_B T). \quad (13)$$

It is indeed well known that kinetic collisionless theory with Maxwellian distributions yields this canonical law, as hydrodynamic equations do. With the potential energy (10), we have  $W/k_B T = z^2/2H^2$  with  $H$  given in (5), yielding a Gaussian density profile — as found in the hydrodynamic picture; (as noted above, the factor of 2 in the argument of the exponential compared to Eq. (8) comes from the non-zero electron temperature.)

But what happens if the distributions are no longer Maxwellian?

### 5.3. Trapped Kappa distributions

Let us assume that the distributions at  $z=0$  are of the form

$$f_0(v) \propto \left[ 1 + \frac{mv^2}{(2\kappa - 3)k_B T_0} \right]^{-(\kappa+1)}, \quad (14)$$

namely a Kappa distribution, which we have now expressed for convenience in terms of the kinetic temperature  $T_0 = m\langle v^2 \rangle / 3k_B$  for a species of mass  $m$ . At altitude  $z$ , we have from (9)

$$f(v, z) \propto \left[ 1 + \frac{mv^2 + 2W}{(2\kappa - 3)k_B T_0} \right]^{-(\kappa+1)} \quad (15)$$

which can be rearranged to give

$$f(v, z) = t^{-(\kappa+1)} \times f_0(v \times t^{-1/2}) \quad (16)$$

with

$$t = 1 + \frac{W}{(\kappa - 3/2)k_B T_0}. \quad (17)$$

Applying dimensional arguments to Eq. (16), it is clear that the kinetic temperature of the new distribution — proportional to the mean of  $v^2$  — will be  $t$  times greater than that of the initial distribution  $f_0$ . The particle number density is deduced in the same way: since it is proportional to  $\int_{-\infty}^{+\infty} dv v^2 f(v)$ , a simple change of variables shows that it must differ from the initial value by the factor  $t^{-(\kappa+1)} \times t^{3/2}$ .

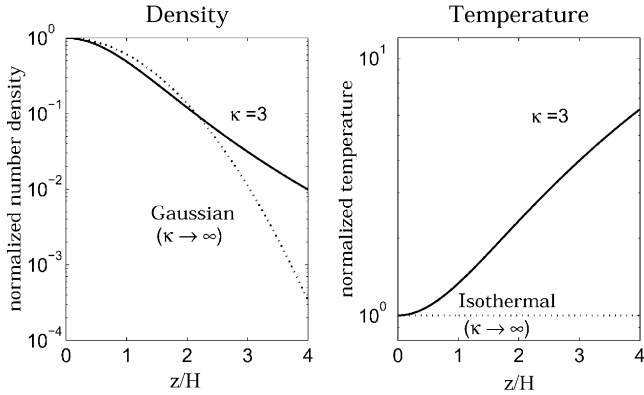


Fig. 5. Vertical density and temperature profiles given by kinetic collisionless theory with a Kappa velocity distribution ( $\kappa = 3$ ), compared to the profiles obtained with a Maxwellian ( $\kappa \rightarrow \infty$ , dotted lines); the latter case is equivalent to the isothermal hydrodynamic picture.

Therefore:

- the number density falls with distance as

$$n \propto t^{1/2-\kappa}; \tag{18}$$

- the kinetic temperature rises as

$$T \propto t \propto n^{\gamma-1}, \tag{19}$$

$$\gamma = 1 - \frac{1}{\kappa - 1/2}. \tag{20}$$

Substituting the potential energy (10) into (17),  $t$  can be written as

$$t = 1 + \frac{z^2}{(2\kappa - 3)H^2} \tag{21}$$

with the “scale height”

$$H = \left[ \frac{2k_B T_0}{3m_i \Omega^2} \right]^{1/2}. \tag{22}$$

Finally, therefore, the density decreases less rapidly than a Gaussian beyond a few scale heights — just as the distribution falls off less steeply than a Maxwellian — while the temperature rises (Fig. 5). The latter result may appear surprising: we are accustomed to relations of the form  $T \propto n^{\gamma-1}$  with index  $\gamma = 1$  (isothermal),  $5/3$  (adiabatic), or somewhere between, but no smaller than unity. The kinetic heat flux is zero, since the distributions are isotropic (in the absence of collisions, there is no collisional heat flux); and yet the temperature rises as the density falls. Why is this so? How is heat transferred? In fact, no heat need be furnished, and, anyway, there no flow. The apparent paradox lies in trying to apply concepts involving thermodynamics and flow to a situation without local equilibrium nor flow; we will return to this point in Section 5.5. The above result may also appear surprising from the kinetic point of view: one might think naïvely that, since particles lose kinetic energy as they rise, they should get “colder” in going upwards. This is not so because the attractive force filters the particles, letting only the most energetic ones escape (Scudder,

1992). In the Maxwellian limit ( $\kappa \rightarrow \infty$ ), one recovers the isothermal Boltzmann profile because in that case all particles are filtered similarly: the potential energy loss en route to  $z$  does not change the slope of the energy distribution, so that the kinetic temperature remains constant (see Fig. 6).

#### 5.4. How does velocity filtration work?

Another way of understanding this effect is to consider a superposition of two Maxwellian distributions at  $z=0$ : a cold one of density  $n_C$  and temperature  $T_C$ , plus a hotter one of density  $n_H$  and temperature  $T_H$  assumed to contribute negligibly to the pressure, so that the kinetic temperature of the whole distribution at  $z = 0$ , equal to  $(n_C T_C + n_H T_H)/(n_C + n_H)$ , is roughly  $T_C$ . Now consider an altitude  $z$  such that the hot particles hardly “see” the potential energy change  $W$ , while the cold ones will consider it as huge, namely,  $k_B T_C \ll W \ll k_B T_H$ . In that case, the filtration is very simple: each Maxwellian distribution is transformed according to Eq. (12) with its own constant temperature, so that the cold and hot densities vary very differently: the hot density hardly decreases because its Boltzmann factor remains close to unity, but the cold density plummets, as its Boltzmann factor does; this yields a mean temperature at  $z$  roughly equal to  $T_H$ . With such a large difference in cold and hot temperatures, the effect seems trivial and the temperature rise from  $T_C$  to  $T_H$  occurs at great altitudes. Indeed, for the mean temperature to be of order  $T_H$ , the hot pressure should exceed the cold one, that is,  $n_H T_H > n_C \exp - (W/k_B T_C) \times T_C$ ; this requires the potential energy  $W$  to be significantly greater than  $k_B T_C$ , which occurs at altitudes of several times the scale height corresponding to the cold temperature.

In fact, the above distribution is not realistic and actual velocity distributions differ significantly from a Maxwellian already at speeds of, say, two or three times the most probable speed (see Fig. 1), so that the temperature rise starts at rather low altitudes. This is illustrated in Fig. 5, which shows the density and temperature profiles calculated for the Kappa distribution ( $\kappa = 3$ ) plotted in Fig. 2, together with the canonical isothermal profiles.

Although actual distributions do have suprathermal tails, their shape is not necessarily Kappa like. What happens in that case? In fact, the rise in temperature as the density falls is expected to be a generic property of distributions having suprathermal tails and subjected to a confining force, as illustrated in Fig. 6 (Scudder, 1992). And it can be proved analytically that this property is shared by all distributions made of a superposition of Maxwellian ones (Meyer-Vernet et al., 1995).

#### 5.5. A recipe for fluid aficionados

We have seen how the ubiquitous non-Maxwellian tails in particle velocity distributions do change the large-scale structure of bound environments: the temperature of each

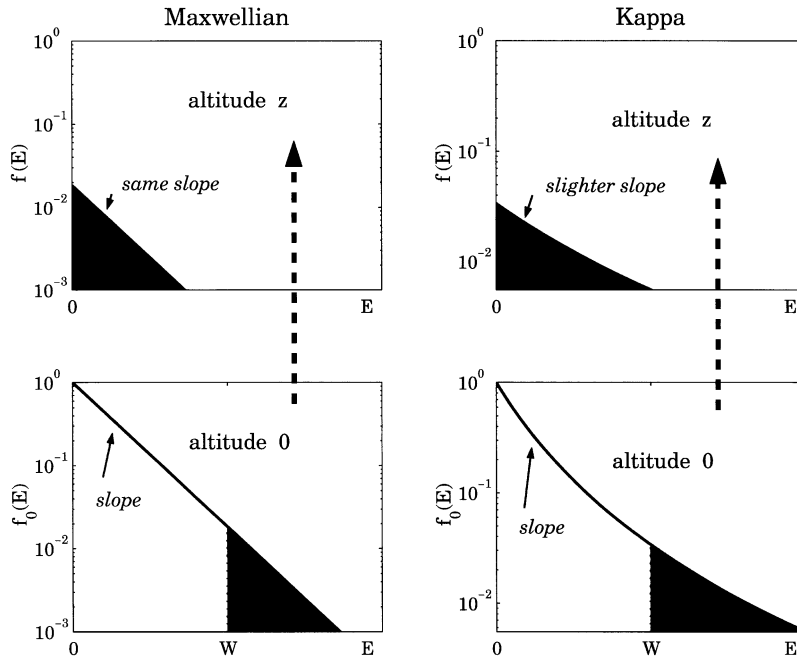


Fig. 6. Velocity filtration by an attracting potential well (see Scudder, 1992). En route to altitude  $z$ , all particles experience the same energy reduction  $W$ , so that the final energy distribution is simply a shifted version of the original. Left-hand side: With a Maxwell distribution, the slope is unchanged and so does the temperature. Right: With a suprathermal tail, whose slope decreases as energy increases, the shifted distribution has a slighter slope than the original at any energy, so that its kinetic temperature is greater.

particle species rises substantially, while its density falls off less rapidly than a Gaussian. For doing so, we have used a kinetic approach which — even without collisions — is somewhat complex, and yet, we made gross simplifications. Introducing into the picture the usual complications that Nature obligingly provides would be far from easy, even with the modern numerical aids; this is the price of doing away with the fluid picture. But need this be so?

With an isotropic velocity distribution, the momentum equation of hydrodynamics applies since the pressure is scalar. And look at Eq. (19): it may be thought of as a formal generalisation of the usual adiabatic relation. This leads us to anticipate that trapped Kappa distributions might be pictured in fluid language by using the simple hydrodynamic equations closed by the relation  $p \propto n^\gamma$ , with the *proviso*  $\gamma < 1$ . Let us see this explicitly. With electrons and ions having similar distributions and temperatures, we may handle them as a single fluid of total pressure  $p = 2nk_B T$ , so that, with  $p \propto n^\gamma$ , the hydrodynamic pressure equation (6) reads

$$\frac{d}{dz} \left( \frac{n}{n_0} \right)^\gamma = -\frac{n}{n_0} \times \frac{3m_i \Omega^2 z}{2k_B T_0} \quad (23)$$

which is easily integrated to yield

$$n \propto \left[ 1 + \frac{1-\gamma}{2\gamma} \frac{z^2}{H^2} \right]^{1/(\gamma-1)} \quad (24)$$

with the “scale height” given in Eq. (22). This is equivalent to the kinetic result, with  $\gamma$  related to  $\kappa$  by Eq. (20).

We conclude that in this case, trapped Kappa distributions can be handled with fluid tools — albeit formally — by putting  $p \propto n^\gamma$  in the hydrodynamic equations. A more general analysis can be found in Scudder (1992). Equations of state having this form are sometimes used in empirical fluid models to fit the observations, and are supposed to make up for some unknown heat transport or source. It is satisfying that we now emerge with a proper justification for doing so, thereby being happily dispensed from imagining an *ad hoc* heat source or abstruse heat transport mechanism. Reassuringly, in the limit  $\gamma \rightarrow 1$  — equivalent to  $\kappa \rightarrow \infty$  in kinetic language — we recover the isothermal equation of state — equivalent to Maxwell distributions in kinetic language.

As we noted, the result found above is extremely surprising from a conventional fluid point of view. First of all, since the usual adiabatic relation holds only *following the motion* of a fluid parcel, it should not apply to the static structure considered here. Secondly, with a scalar pressure and no heat flux, the normal fluid picture leads to the adiabatic index  $\gamma = 5/3$  for particles having three degrees of freedom; one may formally obtain smaller values of  $\gamma$  by assuming more degrees of freedom; but this yields  $\gamma > 1$ .

What happens if one insists in using hydrodynamic equations with  $\gamma > 1$ , as usual? One sees from Eq. (24) that in that case the density — and thus also the temperature —



become negative beyond some distance. Such an unphysical model can be found in the literature, in the context of Saturn’s magnetosphere (Barbosa, 1993, Eqs. (33)–(35). It is reassuring that, in contrast, the kinetic picture does necessarily produce  $\gamma < 1$  because of the ubiquitous supra thermal tails.

## 6. Complications

In trying to highlight the essential physical concepts, I have so far assumed one single ion species, similar isotropic velocity distributions for electrons and ions, and considered a case when the mapping of particle trajectories in phase space was somehow trivial. In practice, however, planetary environments are far more complicated, and these complications cannot be ignored for generating viable models. The detailed calculations require numerical analysis, and the final result will ultimately depend on the mixture which goes into the computer kitchen. Let us try to anticipate on physical grounds how these complications will change the main picture.

### 6.1. Different temperatures

Electrons are so light that when one of them “collides” with an ion — in the Coulomb sense — it rebounds with virtually the same energy. Therefore, collisions between electrons and ions are still less effective to equalise their temperatures than are collisions between like particles to make each distribution Maxwellian. This is why electrons and ions have often very different temperatures, say  $T_e$  and  $T_i$ . How does this complication alter the above results?

Both species must in that case be handled separately, even in the fluid picture. Since they do have similar number densities — neutrality oblige — their pressures are proportional to their temperatures. With different ion and electron pressures, the electric field no longer acts to equalise the forces on ions and electrons; rather it makes these forces proportional to the pressure ones — thus to the temperatures. This holds for the potential energies, too, yielding  $W_i/W_e = T_i/T_e$ . Now, since ions and electrons have opposite electrostatic energies, the total potential energy of ions is related to the centrifugal one as  $W_i = W_c - W_e$ ; we thus have

$$W_i/T_i = W_e/T_e = W_c/(T_i + T_e). \quad (25)$$

Hence, the ratio of the potential energy to the temperature is similar for both species, and is equal to the ratio of  $W_c/2$  (the centrifugal potential of a particle having the average mass) to the average of the ion and electron temperatures.

A similar result holds in the kinetic picture, if both species have similar distributions except for the difference in temperature. Consider Kappa distributions of the form (14) at the equator, for both electrons and ions. We have seen that

for each species, the density and temperature profiles depend only on the ratio of the potential energy  $W$  to the temperature at the equator  $T_0$ . Thus, since the ion and electron densities are everywhere equal, so are the corresponding ratios, whence  $W_i/T_{0i} = W_e/T_{0e}$ . Using  $W_i = W_c - W_e$ , we deduce a result similar to (25). (Note that, by virtue of the relation  $T \propto n^{\gamma-1}$  and of charge neutrality, the ratio of the ion and electron temperatures is everywhere equal to its value at the equator.)

Finally, therefore, if electrons and ions do have different temperatures, the results of the simple model still hold, providing the temperature at the equator is taken as the average of those of ions and electrons.

### 6.2. Anisotropic distributions

The magnetic field introduces a fundamental anisotropy into the problem. Consider, for example, the origin of particles populating a plasma torus. Whatever the details of the creation process, the ultimate source is ionisation of neutrals orbiting at Kepler’s speed in the planet’s equatorial plane. As each new born ion is acted on by the magnetic field, it starts gyrating around it and is put in co-rotation with the planet; it thus acquires a gyro-speed equal to the difference between the co-rotation speed and the Kepler’s one; because the resulting ring-shaped velocity distribution is highly unstable, this is expected to be ultimately converted into a spread in energy perpendicular to the magnetic field; for oxygen ions at Io’s orbit, this amounts to nearly 300 eV — a value much greater than the parallel thermal energy.

This process, among others, tends to produce velocity distributions having different temperatures in the directions parallel and perpendicular to the magnetic field. In that case, we must take account of the approximate invariance of the particle magnetic moment in the co-rotating frame, so that the distributions depend not only on the energy of the particles, but also on their magnetic moment, given by the ratio of the perpendicular kinetic energy  $mv_{\perp}^2/2$  to the value  $B$  of the magnetic field.

The simplest way of generalising our simple model is to assume that the distributions at  $z = 0$  are of the form

$$f_0(v) \propto \left[ 1 + \frac{mv_{\parallel}^2}{(2\kappa - 3)k_B T_{0\parallel}} + \frac{mv_{\perp}^2}{(2\kappa - 3)k_B T_{0\perp}} \right]^{-(\kappa+1)}, \quad (26)$$

that is, a Kappa distribution expressed as a function of the kinetic temperatures in the directions parallel and perpendicular to the magnetic field, for a species of mass  $m$ . With all trajectories at  $z$  connecting to  $z = 0$  (since both the potential energy and the magnetic field are increasing with  $z$ ), the distributions evolve along field lines as  $f(v_{\parallel}, v_{\perp}, z) = f_0(v_{0\parallel}, v_{0\perp})$  with conservation of energy and magnetic moment, whence

$$m(v_{\parallel}^2 + v_{\perp}^2)/2 + W = m(v_{0\parallel}^2 + v_{0\perp}^2)/2, \quad (27)$$

$$v_{\perp}^2 = v_{0\perp}^2 \times B/B_0. \quad (28)$$

Substituting into  $f_0$  the speeds  $v_{0\parallel}$  and  $v_{0\perp}$  as functions of  $v_{\parallel}$  and  $v_{\perp}$  and rearranging the terms, we find the following simple generalisation of the isotropic result (16):

$$f(v_{\parallel}, v_{\perp}, z) \propto t^{-(\kappa+1)} \times f_0(v_{\parallel} \times t^{-1/2}, v_{\perp} \times t^{-1/2} \times b^{1/2}) \quad (29)$$

with

$$t = 1 + \frac{W}{(\kappa - 3/2)k_B T_{0\parallel}}, \quad (30)$$

$$b = B_0/B + T_{0\perp}/T_{0\parallel}(1 - B_0/B). \quad (31)$$

We deduce as previously the density and temperature profiles from dimensional analysis:

$$n \propto t^{1/2-\kappa}/b, \quad (32)$$

$$T_{\parallel} \propto t \propto (nb)^{\gamma-1}, \quad (33)$$

$$T_{\parallel}/T_{\perp} \propto b. \quad (34)$$

Thus, the temperature variation found previously still holds, but only for the parallel temperature; this is not surprising since the centrifugal effect filtering the particles acts in that direction. As  $z$  increases, the magnetic field rises, and the perpendicular temperature gets closer to the parallel one. The anisotropy also changes the density profile, making it steeper when the perpendicular temperature is greater than the parallel one. It is reassuring that these results reduce to those of our elementary model if either the distribution is isotropic or the magnetic field is constant.

In the Maxwellian limit ( $\kappa \rightarrow \infty$ ),  $T_{\perp}$  still comes closer to  $T_{\parallel}$  as  $z$  increases, but the parallel temperature remains constant (see Huang and Birmingham, 1992). Note in passing that when the particle thermal energy is not small compared to their co-rotation energy, the average mirror force resulting from the anisotropy plays a role. When the magnetic and spin axes do not coincide, this effect shifts slightly the equilibrium position. And if ions and electrons have different anisotropies, an additional electric field arises to cancel the charge imbalance that this difference tends to produce, as first shown by Alfvén and Fälthammar (1963). Finally, in that case the problem of determining the accessibility of trajectories in phase space becomes rather tricky (Chiu and Schulz, 1978), and its solution requires subtle techniques (Liemohn and Khazanov, 1998).

Looking at Fig. 5 and comparing to Eq. (32), we see that for the anisotropy to have a significant effect,  $b$  should differ from 1 by a substantial factor, which requires that both the temperature anisotropy at the equator *and* the magnetic field variation be substantial.

### 6.3. A mixture of ions

In contrast to the interplanetary medium which is mainly made up of protons and electrons, planetary environments

are often a rich mixture of various species. How does this alter the picture? In that case, the electric field compensating for the electron lightness can be estimated by handling the ion mixture as a single “average” ion species of mass  $\langle m \rangle$  and charge  $\langle Z \rangle e$ , whose centrifugal potential energy  $\langle W_c \rangle$  is given by substituting the mass  $\langle m \rangle$  in Eq. (4). Let us assume that all species have similar energy distributions with the same temperature (if this is not so, the results can be generalised as outlined in Section 6.1). Since in that case the electric field acts to equalise the forces on electrons and ions, the potential energy of electrons,  $W_e$ , is equal to that of the average ion,  $\langle W_c \rangle - \langle Z \rangle W_e$ , whence  $W_e = \langle W_c \rangle / (1 + \langle Z \rangle)$ . The electrostatic potential energy  $W_i$  of an ion of charge  $Z_i e$  is of opposite sign and  $Z_i$  times greater, that is,  $-Z_i \langle W_c \rangle / (1 + \langle Z \rangle)$ . The total potential energy of that ion of mass  $m_i$  is thus given by

$$W_i = \langle W_c \rangle \times \left[ \frac{m_i}{\langle m \rangle} - \frac{Z_i}{1 + \langle Z \rangle} \right]. \quad (35)$$

This result has several interesting consequences. First, we see that for ions lighter than average, the bracket may be very small and even negative. This means that not only are lighter species inefficiently trapped — a rather trivial result — but their density can even rise with distance when the electrostatic force dominates. We will return to this point later.

Consider now ions being heavier than average. In that case, the first term in the potential energy (35) dominates, making it roughly  $(m_i/\langle m \rangle)^{1/2}$  times greater than average, so that the density profile decreases faster than average: the heavier the ion, the more it is bound. This result, however, as the one above, is not a privilege of non-Maxwellian distributions (see Angerami and Thomas, 1964). But consider the temperature, which is proportional to the parameter  $t$  (Eq. (17)) relative to that ion: as soon as the potential energy term dominates in the expression of  $t$  — in practice this occurs beyond a few scale heights of that species — the ion temperature (proportional to  $t$ , thus to  $W_i$ ) becomes proportional to its mass: the heavier the ion, the greater the potential energy, and therefore the more effective the filtration making the temperature rise.

Finally, therefore, the kinetic calculation makes an interesting prediction: the temperature of non-Maxwellian ions heavier than average should increase as their potential energy, proportional to their mass: for example, in a proton-dominated environment, oxygen ions should be 16 times hotter than average — a result first noted by Scudder (1992) in a quite different context: filtration by the solar gravitational field.

## 7. When gravitation dominates the picture

While gravitation is negligible sufficiently far from planets, this is not so at closer distances. One must then take into

account the gravitational potential energy in addition to the centrifugal one, that is

$$W_{C+G} = -m\Omega^2(r \cos \lambda)^2/2 - mMG/r + \text{constant} \quad (36)$$

for a particle of mass  $m$  at radial distance  $r$  and latitude  $\lambda$ , in a frame of reference rotating with the planet, where we no longer restrict ourselves to small latitudes (Fig. 4). At first sight, this should enable one to determine the particle distributions along magnetic field lines in a straightforward way. In fact, it turns out that the problem is not that simple, because along field lines going farther than the “Roche distance”  $r_c$  defined in (3), the net acceleration has not everywhere the same direction. To see this, we substitute in (36) the equation of a field line crossing the equator at distance  $L$ ,  $r = L \cos^2 \lambda$ , and calculate the derivative of  $W_{C+G}$  with respect to  $r$  or to  $\lambda$ ; one sees that if  $L \geq r_c$ , then the potential energy has a maximum (one on each side of the equator) separating the foot side of the line — where particles are attracted towards the planet — from the equator side — where particles are pulled towards the equator. Only particles having sufficient energy are able to cross this point. Therefore, a careful analysis of particle orbits is necessary to determine the velocity range of particles capable of reaching a given position when starting from the “source” region where the boundary conditions are defined (see for example Goertz, 1976; Lemaire, 1976). As already mentioned, this problem is especially tricky if the velocity distributions are anisotropic (Liemohn and Khazanov, 1998).

A considerable simplification arises close enough to the planet that gravity is strongly dominant. In that case, gravity confines particles near the planet in much the same way as the centrifugal force does near the equator. Therefore our simple model applies, just replacing the centrifugal potential increase by the gravitational one

$$W_G = -mMG(1/r - 1/r_0) \quad (37)$$

$r_0$  being the reference level near the foot of the field line, where the velocity distributions are assumed to be known. This reference level is taken as the altitude where the medium is dilute enough that the mean free paths just exceed the scale heights. One must keep in mind that the formal similarity between the centrifugal and gravitational problems holds only for *isotropic* distributions (or when the magnetic field variation can be neglected): indeed, while the magnetic field value *increases* away from the equator, it *decreases* away from the planet, so that the calculations should be modified because of the accessibility problems already mentioned.

With this *proviso*, the simple results found for plasma tori hold in planetary plasmaspheres, as in other gravitationally bound environments. And indeed, velocity filtration has been recently proposed to explain the strong temperature rise with altitude observed in the outer plasmasphere of the Earth, where the plasma density drops abruptly to the near void of the magnetospheric cavity (Pierrard and Lemaire, 1996).

At altitudes  $z$  sufficiently close to a body of radius  $R$  that the distances may be approximated by  $r_0 \approx R$  and  $r \approx R+z$ , the gravitational potential (37) reduces to  $W_G \approx mMGz/R^2$ . In that case, comparing to the centrifugal value (4), we see that the formulae derived for centrifugal binding also hold for gravitational binding providing  $z^2/H^2$  is replaced by  $z/H_G$  with the gravitational scale height

$$H_G = \frac{k_B T_0}{mMG/R^2}. \quad (38)$$

## 8. A kinetic picture of winds

We have so far considered bound structures shaped along closed magnetic field lines. Consider now the particles channelled along open field lines emerging from polar regions. As we noted, although collisions are generally important in the close vicinity of the body, they may be neglected beyond the distance where the mean free paths exceed the scale height; this is taken as the reference level — referred to as the “exobase” in the kinetic jargon; in the Earth’s environment, this corresponds to an altitude, in round figures, of 1000 km.

### 8.1. Simple picture of a planetary polar wind

Particles following open magnetic field lines can escape from the body if their kinetic energy at the exobase does exceed their binding potential energy. This problem recalls Jeans’ theory of neutral gas evaporation (Jeans, 1954) with, however, a crucial difference: as emphasised by Dessler and Cloutier (1969) in the first kinetic study of what is generally referred to as the “polar wind”, the light ions are not bound at all, because they are pulled outwards by an electric force which exceeds the gravitational attraction. This comes about because the electrostatic field preserving charge neutrality in static equilibrium halves the gravitational attraction on the “average” ion (for equal temperatures), as discussed in Section 6.3. Since the dominant ion just above the Earth’s “exobase” is oxygen — of mass  $16m_p$ , the outward electric force is equal to  $8m_pMG/r^2$ . Now consider light ions, such as protons; since the gravitational attraction on them is 8 times smaller than this electrostatic force, they are pushed outwards by a net force equal to  $7m_pMG/r^2$ : this is the essence of the “polar wind”.

At this point, the fluid and kinetic pictures should agree, although the key role of the electric field emerges less clearly in the fluid scheme. But this is not the whole story. One might think that this acceleration of light ions should stop at some altitude where the heavy ions responsible for the large electric field no longer dominate the composition. Indeed, the density of oxygen ions falls off rapidly outwards since their large mass makes their scale height (38) very small; and as soon as protons dominate, the electric force should reduce to one-half the gravitational attraction on them, so that they should no longer be pulled outwards. In fact, it

turns out that this is not so because this reduced electrostatic field was calculated for a static equilibrium, and is no longer valid when a wind is blowing. Indeed, if the electrostatic force were reduced to half the gravitational attraction on the protons at altitudes where they dominate, then the corresponding potential energies would be too small to correct the tendency of electrons to escape faster than ions because of their greater random speed. Thus the source of the wind would charge positively. To ensure charge equilibrium, the electric field must be great enough to bind the electrons sufficiently strongly to make their outward flux balance the proton one.

We conclude that the electrostatic field remains large, even beyond the altitude where protons become dominant (Lemaire and Scherer, 1973). In addition, since the bulk speed increases outwards, the proton density must decrease with altitude to preserve a constant flux; this extends the region where heavy ions dominate the composition. The net result is that the electric field keeps the large value calculated above out to about 5000 km altitude.

Let us try to estimate the wind speed  $V$ . To a first approximation, the bulk kinetic energy of the protons comes ultimately from the gain in potential energy between the exobase and the altitude of 5000 km, that is

$$V^2/2 \approx 7MG(1/r_0 - 1/r). \quad (39)$$

Putting the exobase at 1000 km above the planetary surface and substituting the mass of the Earth ( $6 \times 10^{24}$  kg) and its radius ( $6.4 \times 10^6$  m), we find a wind speed of about 16 km/s. It is gratifying — but not necessarily significant — to see that this value is in the range of proton speeds observed in the Earth's polar wind. We have neglected the thermal contribution to the energy balance and the bulk speed at  $r_0$ , but this hardly changes the final result since the kinetic energy of the wind directed motion is much greater than these contributions. Consider now what happens to the heavy ions. We have seen that the net force acting on them (as on the electrons) is directed inwards; but those having a kinetic energy greater than the potential energy at the exobase can escape; so, the oxygen leaks away, with a bulk speed much smaller than its thermal speed.

### 8.2. Pushing the wind with a suprathermal electron tail

How does the shape of the particle velocity distributions enter into this picture? We have seen that the electrostatic field tends to trap the electrons, so that only those having a kinetic energy greater than their potential energy at the exobase can escape; in other words, the high-speed particles are responsible for the lion's share of the electron flux. Thus if the electron velocity distribution has an excess of energetic particles — even a small one — this tends to increase substantially the escaping electron flux, thereby charging the atmosphere positively. As a consequence, the electric field rises in order to trap more electrons and keep their escaping flux equal to the proton one. And in turn

this greater electric field accelerates the protons outwards, thereby increasing the wind speed. A similar effect has been proposed in the context of the solar wind — which in a sense is simpler because a single ion species dominates the composition (see Maksimovic et al., 1997b; Meyer-Vernet, 1999).

It is worth noting that all these results must be taken with a pinch of salt: we have made gross simplifications in trying to extract the essence of the physics. More realistic calculations and numerical aids are necessary to build viable models (see for example Pierrard, 1997).

## 9. Final remarks and questions

To preserve the reader's morale, we have swept under the carpet a number of disturbing — albeit fundamental — questions.

First of all, the concept of temperature lies at the heart of classical macroscopic physics. But what does it mean in the absence of thermodynamic equilibrium? Indeed, all our instinctive and academic knowledge of it is based on some kind of local equilibrium. In the kinetic picture, the temperature quantifies the variance of the statistical distribution of velocities as  $T = m\langle v^2 \rangle / 3k_B$ ,  $v$  being the speed in the frame where the mean velocity is zero. But in contrast to the equilibrium case where this quantity (together with the number density and mean velocity) is sufficient to characterise the distribution, here the temperature is merely one particular moment among others. Suppose we wish to compare our calculations with observation, which would be quite legitimate — and even eminently desirable. What should we do? Unfortunately, with non-Maxwellian distributions, the measured temperature depends on the measuring device because most detectors are sensitive to a very restricted velocity range and have bias which depend on the particle velocity; many detectors turn out to merely measure an approximation of one moment of the distribution, whose relation to the kinetic temperature depends on the distribution itself. Worse still, many devices are built under the hidden assumption of equilibrium and one is at risk of being fooled by deeply ingrained prejudices. (An apt example of the prejudices of the author of this paper is provided in the caption of Fig. 6, where we deduce in a cavalier way the temperature behaviour from the slope of the logarithm of the energy distribution; in fact, this reasoning would be correct only with a Maxwellian, and our excuse is that we used it only for illustrative purposes.)

This brings us to a second question: is the temperature increase resulting from velocity filtration a privilege of the kinetic temperature, or does it hold also for other related quantities — which would make this effect more fundamental? The answer is yes: with a Kappa distribution, relation (19) found between density and temperature holds for any generalised “temperature”  $T_q$  defined from any scalar

moment of the distribution,  $M_q = \int d^3v v^q f(v)$  as

$$\frac{k_B T_q}{m} = \left[ \frac{M_q}{nC_q} \right]^{2/q} \quad (40)$$

where  $C_q$  is defined below, so as to make all  $T_q$  equal to the bona fide temperature if the distribution is Maxwellian (Meyer-Vernet et al., 1995). The moment  $M_0 = n$  is the number density, and  $M_2$  is proportional to the pressure, so that  $T_2$  is the usual kinetic temperature; here the moments are defined in the frame where the mean velocity is zero, and

$$C_q = (q+1)!!(q \text{ even}), \quad (41)$$

$$C_q = (2^{q/2+1}/\sqrt{\pi})[(q+1)/2]!(q \text{ odd}) \quad (42)$$

where  $q > -3$ . The larger the index  $q$ , the greater the speed of the particles being responsible for that “temperature”. In this way, the mean random speed is related to  $T_1$  as  $\langle v \rangle = (8k_B T_1/\pi m)^{1/2}$ , while the mean-square speed is  $\langle v^2 \rangle = 3k_B T_2/m$ ; the Debye length, which depends on the mean-square inverse speed, is related to  $T_{-2}$  as  $L_D = (\epsilon_0 k_B T_{-2}/n e^2)^{1/2}$  (see Meyer-Vernet, 1993); this enables one to generalise to arbitrary distributions these canonical formulae normally used for Maxwellians.

It is somewhat reassuring that the temperature increase produced by velocity filtration is not a privilege of the kinetic temperature defined from the spread in particle speeds. This means that devices having different bias — as those measuring the Debye length or the random flux of particles — should find a similar “temperature” increase as an ideal device measuring the bona fide kinetic temperature. In the particular case of Ulysses in the Io plasma torus, the measured electron “temperature” was in fact roughly  $T_{-2}$ .

We have discussed the effects of suprathermal tails in velocity distributions because, as a rule, space plasmas have too much suprathermal particles. But what would happen if some distribution would manage by whatever tortuous means to have less fast particles than a Maxwellian? The reasoning of Fig. 6 would then suggest a temperature decrease with altitude for a bound structure. Could such tricky effects be observed in special cases?

Finally, just as the fluid models of space plasmas can be criticised because the closure schemes are often inadequate due to the rarity of collisions, so the kinetic collisionless picture might be criticised because the medium is not fully collisionless. This brings up one more question. How are the effects discussed in this paper altered when collisions are not fully negligible? A reassuring point is that these effects are based on supra thermal particles, which are minimally affected by collisions — by virtue of the strong increase of the particle free path with energy. But this latter property suggests that the simple picture of all particles being collisionless beyond the same level (the “exobase”, defined from the mean free path), may be oversimplified (see Brandt and Cassinelli, 1966). More generally, the transition from the

fully collisional feet of the field lines to the virtually collisionless plasma encountered farther out is far from being properly understood. A correct picture should involve some hybrid scheme (see Dorelli and Scudder, 1999) or simulations (Pantellini and Landi, 2000), and this might reserve a number of ingenious surprises.

## Acknowledgements

I would like to thank J. F. Lemaire for bringing to my attention a number of references. Special thanks are due to F. Meyer who drew the pictures on which Fig. 3 is based.

## References

- Alfvén, H., Fälthammar, C.G., 1963. *Cosmical Electrodynamics*. Clarendon Press, Oxford, U.K.
- Angerami, J.J., Thomas, J.O., 1964. *Studies of Planetary Atmospheres* 1. The distribution of electrons and ions in the Earth’s exosphere. *J. Geophys. Res.* 69, 4537–4560.
- Bagenal, F., 1994. Empirical model of the Io plasma torus. I. Voyager measurements. *J. Geophys. Res.* 99, 11,043–11,062.
- Barbosa, D.D., 1993. Thermal structure of ions and electrons in Saturn’s inner magnetosphere. *J. Geophys. Res.* 98, 9335–9343.
- Brandt, J.C., Cassinelli, J.P., 1966. *Interplanetary gas XI. An exospheric model of the solar wind*. *Icarus* 5, 47–63.
- Chandrasekhar, S., 1942. *Principles of Stellar Dynamics*. University of Chicago Press.
- Chiu, Y.T., Schulz, M., 1978. Self-consistent particle and parallel electrostatic field distributions in the magnetospheric-ionospheric auroral region. *J. Geophys. Res.* 83, 629–642.
- Christon, S.P., et al., 1988. Energy spectra of plasmashet ions and electrons from 50 eV/e to 1 MeV during plasma temperature transitions. *J. Geophys. Res.* 93, 2562–2572.
- Collier, M.R., 1993. On generating Kappa-like distribution functions using velocity space Lévy flights. *Geophys. Res. Lett.* 22, 303–306.
- Cummings, W.D., Dessler, A.J., Hill, T.W., 1980. Latitudinal oscillations of plasma within the Io torus. *J. Geophys. Res.* 85, 2108–2114.
- Dessler, A.J., Cloutier, P.A., 1969. Discussion of letter by Peter M. Banks and Thomas E. Holzer, “The polar wind”. *J. Geophys. Res.* 74, 3730–3733.
- Dorelli, J.C., Scudder, J.D., 1999. Electron heat flow carried by Kappa distributions in the solar corona. *Geophys. Res. Lett.* 26, 3537–3540.
- Doyle, A.C., 1927. *The Casebook of Sherlock Holmes: the Adventure of Shoscombe Old Place*. Penguin Books, London.
- Fort, J., Gonzalez, J.A., Llebot, J.E., Saurina, J., 1999. Information theory and blackbody radiation. *Contemp. Phys.* 40, 57–70.
- Gledhill, J.A., 1967. Magnetosphere of Jupiter. *Nature* 214, 155–156.
- Goertz, C.K., 1976. Plasma in the Jovian Magnetosphere. *J. Geophys. Res.* 81, 2007–2014.
- Hinton, F.L., 1983. Collisional transport in plasma. In: Galeev, A.A., Sulan, R.N. (Eds.), *Basic Plasma Physics*. North-Holland, Amsterdam, pp. 147–197.
- Huang, T.S., Birmingham, T.J., 1992. The polarisation electric field and its effect in an anisotropic rotating plasma. *J. Geophys. Res.* 97, 1511–1519.
- Jeans, J.H., 1954. *The Dynamical Theory of Gases*. Dover, New York.
- Lemaire, J., 1974. The ‘Roche-limit’ of ionospheric plasma and the formation of the plasmopause. *Planet. Space Sci.* 22, 757–766.
- Lemaire, J., 1976. Rotating ion-exospheres. *Planet. Space Sci.* 24, 975–985.
- Lemaire, J.F., 1999. Hydrostatic equilibrium and convective stability in the plasmasphere. *JASTP* 61, 867–878.

- Lemaire, J., Scherer, M., 1973. Kinetic models of solar and polar winds. *Rev. Geophys. Space Phys.* 11, 427–468.
- Liemohn, M.W., Khazanov, G.V., 1998. Collisionless plasma modeling in an arbitrary potential energy distribution. *Phys. Plasmas* 5, 580–589.
- Maksimovic, M., Pierrard, V., Riley, P., 1997a. Ulysses electron distributions fitted with Kappa functions. *Geophys. Res. Lett.* 24, 1151.
- Maksimovic, M., Pierrard, V., Lemaire, J., 1997b. A kinetic model of the solar wind with Kappa distribution functions in the corona. *Astron. Astrophys.* 324, 725.
- Maurice, S., 1994. Thesis. Université Paris 7.
- Meyer-Vernet, N., 1993. Aspects of Debye shielding. *Am. J. Phys.* 61, 249–257.
- Meyer-Vernet, N., Hoang, S., Moncuquet, M., 1993. Bernstein waves in the Io plasma torus: A novel kind of electron temperature sensor. *J. Geophys. Res.* 98, 21,163.
- Meyer-Vernet, N., Moncuquet, M., Hoang, S., 1995. Temperature inversion in the Io plasma torus. *Icarus* 116, 202–213.
- Meyer-Vernet, N., 1999. How does the solar wind blow? A simple kinetic model. *Eur. J. Phys.* 20, 167–176.
- Moncuquet, M., Meyer-Vernet, N., Hoang, S., 1995. Dispersion of electrostatic waves in the Io plasma torus and derived electron temperature. *J. Geophys. Res.* 100, 21,697.
- Moncuquet, M., 1997. Thesis. Université Paris 7.
- Montgomery, D.C., Tidman, D.A., 1964. *Plasma Kinetic Theory*. McGraw-Hill, New York.
- Pantellini, F., Landi, S., 2000. A simulation method for semicollisional plasmas. *Astrophys. Space Sci.*, in press.
- Pierrard, V., Lemaire, J., 1996. Lorentzian ion exosphere model. *J. Geophys. Res.* 101, 7923–7934.
- Pierrard, V., 1997. Fonction de distribution des vitesses des particules s'échappant de l'ionosphère. Thesis. Université Catholique de Louvain, Belgium.
- Scudder, J.D., Olbert, S., 1979. A theory of local and global processes which affect solar wind electrons, I. The origin of typical 1 AU velocity distributions. *J. Geophys. Res.* 84, 2755.
- Scudder, J.D., Olbert, S., 1983. The collapse of the local, Spitzer-Härm formulation and a global-local generalization for heat-flow in a inhomogeneous, fully ionized plasma. In: Neugebauer, M. (Ed.), *Solar Wind Five*, NASA Conf. Pub., vol. 2280, pp. 163–181.
- Scudder, J.D., 1992. On the causes of temperature change in inhomogeneous low-density astrophysical plasmas. *Astrophys. J.* 398, 299–318.
- Shoub, E.C., 1983. Invalidity of local thermodynamic equilibrium for electrons in the solar transition region. I. Fokker-Planck results. *Astrophys. J.* 266, 339–369.
- Spitzer Jr., L., 1962. *Physics of Fully Ionized Gases*. Interscience Pub., New York.
- Thomas, N., Lichtenberg, G., 1997. The latitudinal dependence of ion temperature in the Io plasma torus. *Geophys. Res. Lett.* 24, 1175–1178.
- Treumann, R.L., 1999. Generalized Lorentzian thermodynamics. *Phys. Scri.* 59, 204.
- Vasyliunas, V.M., 1968. A survey of low-energy electrons in the evening sector of the magnetosphere with Ogo 1 and Ogo 3. *J. Geophys. Res.* 73, 2839–2885.